

# Influence of the mineralogical composition on the self-potential response to advection of KCl concentration fronts through sand

Alexis Maineult,<sup>1,2</sup> Laurence Jouniaux,<sup>1</sup> and Yves Bernabé<sup>1</sup>

Received 7 September 2006; revised 1 November 2006; accepted 22 November 2006; published 23 December 2006.

[1] We measured the self-potential (SP) response to advective transport of KCl concentration fronts through two laboratory-scale sand-bodies with different mineralogical composition. In pure quartz sand, the amplitude and polarity of the SP signals agreed with a previously published model. In sand containing 3% potassic feldspars and 1% micas and clays, the shape of the SP response differed significantly: the amplitude was much larger than the model prediction and a change in polarity occurred after the passage of the front. Furthermore, the KCl concentration in the effluent was strongly reduced. We suggest that the minor mineral phases reacted with the  $K^+$  ions, trapping them during the front passage and releasing them later. Even though the reactions involved are not fully identified to date, this study demonstrates that even small amounts of chemically active mineral phases, such as micas or clays, can significantly influence the SP signals. **Citation:** Maineult, A., L. Jouniaux, and Y. Bernabé (2006), Influence of the mineralogical composition on the self-potential response to advection of KCl concentration fronts through sand, *Geophys. Res. Lett.*, 33, L24311, doi:10.1029/2006GL028048.

## 1. Introduction

[2] Self-potential (SP) monitoring is a geophysical method based on the measurement of the natural voltage fields present in the subsurface. It has been intensively used in recent subsurface studies, even though the simultaneous action of many different SP sources, such as variations in groundwater flow, chemistry or temperature [e.g., *Corwin and Hoover, 1979*], can make the interpretation difficult in terms of fluid velocity and composition. To better characterize these processes, sand-box experiments involving reproducible, controlled sources have been conducted in the laboratory [*Ahmad, 1964; Maineult et al., 2004, 2005, 2006; Suski et al., 2004; Naudet and Revil, 2005*]. In previous works focusing on the SP response to advective transport of NaCl and FeCl<sub>2</sub> concentration fronts [*Maineult et al., 2004, 2005, 2006*], we found that, to first order, the SP signals could be modeled as the sum of: 1) an electrokinetic term, related to local changes of the electrokinetic coupling coefficient with varying fluid concentration, and 2) a fluid junction potential term, caused by the presence of a concentration gradient. Noting that the second term should vanish when ionic species with identical mobilities

are used, we tried to test this prediction by running advective transport experiments using a KCl solution (the mobility of  $K^+$  is equal to 96% of the mobility of  $Cl^-$ ). However the observations appeared to contradict this theoretical prediction. This unexpected discrepancy led us to perform a new set of KCl advection experiments using a 100% pure quartz sand instead of the previously employed sand, which contained small amounts of feldspars, clays and micas. The results reported here suggest that the anomalous SP signals can be attributed to chemical reactions between  $K^+$  and the minor minerals.

## 2. Background

[3] Fluid flow through a porous medium produces a downstream motion of the counter-ions in excess near the charged pore-walls, resulting in a net charge separation and, consequently, in the generation of the so-called electrokinetic field. Assuming no surface conductivity, the electric and hydraulic potentials  $U_e$  (in V) and  $H$  (in m) are related to each other by the Helmholtz-Smoluchowski equation:

$$\nabla U_e = L^* \nabla H = \frac{\rho g \varepsilon \zeta}{\eta \sigma} \nabla H \quad (1)$$

where,  $\rho$ ,  $\varepsilon$ ,  $\eta$  and  $\sigma$  are the density ( $kg\ m^{-3}$ ), dielectric constant ( $F\ m^{-1}$ ), viscosity ( $Pa\ s$ ) and electrical conductivity ( $S\ m^{-1}$ ) of the fluid,  $g$  the gravity acceleration ( $m\ s^{-2}$ ) and  $L^*$  the electrokinetic coupling coefficient ( $V\ m^{-1}$ ). The so-called “zeta-potential”  $\zeta(V)$  depends on the geochemical properties of the rock, and on the fluid composition and concentration [e.g., *Ogilvy et al., 1969; Ishido and Mizutani, 1981; Lorne et al., 1999; Guichet and Zuddas, 2003; Hase et al., 2003*]. Equation (1) implies that any change in the fluid concentration can modify the electrokinetic potential.

[4] As ionic species diffuse along a concentration gradient, a net charge separation occurs if the anion and cation mobilities are different, thus generating a counteracting electrical field. The junction potential  $U_j$  (V) obeys the Planck-Henderson equation:

$$\nabla U_j = \varphi \frac{RT}{Ae} \frac{\nabla(\sigma_- - \sigma_+)}{\sigma_- + \sigma_+} \quad (2)$$

where  $\sigma_-$  and  $\sigma_+$  are the anionic and cationic electrical conductivities (such as  $\sigma_- + \sigma_+ = \sigma$ ),  $\varphi$  the porosity,  $T$  the absolute temperature (K),  $R$  the molar gas constant ( $8.314\ J\ mol^{-1}\ K^{-1}$ ),  $A$  Avogadro’s number ( $\approx 6.022 \cdot 10^{23}\ mol^{-1}$ ) and  $e$  the absolute electron charge ( $\approx 1.602 \cdot 10^{-19}\ C$ ). In the

<sup>1</sup>Institut de Physique du Globe de Strasbourg, CNRS UMR 7516, Université Louis Pasteur, Strasbourg, France.

<sup>2</sup>Now at Institut de Physique du Globe de Paris, Paris, France.

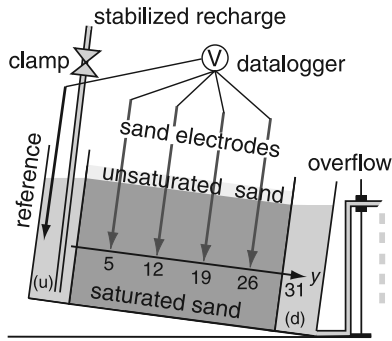


**Figure 1.** Experimental set-up. Flow is generated by tilting the sandbox while maintaining the water levels in the upstream (u) and downstream (d) reservoirs constant. The electrodes, connected to the data-logger, are represented as downward pointing arrows. Their  $y$ -position (in cm) are also indicated.

case of a symmetric, monovalent, binary salt such as NaCl or KCl, equation (2) can be simplified as:

$$\nabla U_j = \alpha^* \frac{\nabla C}{C} = \phi \frac{RT}{Ae} \frac{u_- - u_+}{u_- + u_+} \frac{\nabla C}{C} \quad (3)$$

where  $\alpha^*$  is the junction coupling coefficient in a porous medium (V),  $C$  the salt concentration ( $\text{mol m}^{-3}$ ), and  $u_-$  and  $u_+$  the ionic mobilities ( $\text{m}^2 \text{s}^{-1} \text{V}^{-1}$ ) of anions and cations, respectively.

### 3. Materials and Method

#### 3.1. Flow-Through Sand-Box

[5] We performed the experiments reported here in the sand-box described in detail by *Maineult et al.* [2004, 2005] (Figure 1). Briefly, a rectangular container ( $44.25 \times 23.75 \times 26.50$  cm) was divided into three hydraulically connected compartments. The end-reservoirs (5.7- and 6.1-cm long) were used to control the flow, while the 31-cm long inner one was filled up with a 21-cm height water-saturated sand-body. Precautions were taken to ensure packing homogeneity and avoid air trapping.

[6] A uniform, one-dimensional flow field was produced by tilting the container by an angle of  $4.4^\circ$  (corresponding to a mean hydraulic gradient  $\nabla H = -7.7\%$ ) while maintaining the water level in each end-reservoir constant at 20 cm from the box bottom. Note that about 60 liters of water were circulated through the sand in a closed circuit for several days before the experiment, to reach steady-state flow and chemical equilibrium conditions. After establishing steady-state flow (i.e. stabilized flowrate, conductivity and electrical potential differences), we generated a sharp concentration pulse at time  $t = 0$  by quickly adding and stirring  $6 \text{ cm}^3$  of saturated KCl solution in the upstream reservoir. This volume was small enough to minimize the perturbation of flow (the resulting transitory, upstream water level increase was only  $\approx 0.5$  mm). Generating the pulse took less than 10 s. We then stirred the upstream reservoir every 2 minutes to ensure a homogeneous upstream solution. This procedure produced a sharp concentration front followed by an exponentially decaying tail. Note that the device was

switched to an open-circuit just before the injection, i.e., the fluid passed through the sand was not used again, to avoid any contamination of the recharge reservoir by KCl.

[7] We measured the electrical potential differences (or EPDs) between a reference electrode placed in the upstream reservoir and four electrodes inserted at half height in the sand body, along a median, longitudinal line, at distances  $y$  equal to 5, 12, 19 and 26 cm from the upstream reservoir (Figure 1). We used the small-size (i.e., 4 mm in diameter), copper-copper sulfate, unpolarisable electrodes described by *Maineult et al.* [2004]. To remove the intrinsic potential of each electrode and the constant electrokinetic signal produced by the steady-state flow of the primary fluid (i.e., the fluid circulating before the injection), the EPD signals were reduced by their individual initial value (all curves shown hereafter thus represent variations with respect to the initial steady-state flow of the primary fluid).

#### 3.2. Sands

[8] The S4M sand from Haguenau, France, contains 96% quartz, about 3% potassic feldspars (microcline and sanidine) and slightly more than 1% micas and clay minerals (essentially altered biotite, muscovite and illite). For the non-clay minerals, the grain diameter ranges in the interval  $200\text{--}400 \mu\text{m}$ , with a mean of  $292 \mu\text{m}$ . The porosity  $\phi$  of several similarly packed sand samples was determined by dry and water-saturated weighting and ranged between 36.5 and 37.0%. By means of a column permeameter and *Jouniaux et al.*'s [2000] electrokinetic measurement system, we measured a hydraulic permeability between 20 and  $22 \cdot 10^{-12} \text{ m}^2$ . We measured the electrical conductivity of the saturated sand  $\sigma_r$  for different KCl solutions with conductivity  $\sigma$  ranging between 2.5 and  $100 \text{ mS m}^{-1}$ . The electrical formation factor  $F$  and the surface conductivity  $\sigma_s$ , defined by  $\sigma_r = \sigma/F + \sigma_s$ , were equal to 4.70 and  $0.6 \text{ mS m}^{-1}$ , respectively.

[9] The NE34 (SIFRACO) sand from Nemours, France, is 100% pure quartz. We did not observe any traces of clays or micas. The grain diameter ranges between 75 and  $320 \mu\text{m}$ , with a mean of  $198 \mu\text{m}$ . The porosity is about 36% and the permeability  $17.5 \cdot 10^{-12} \text{ m}^2$ . The formation factor was found equal to 4.90 (with  $\sigma$  between 50 and  $500 \text{ mS m}^{-1}$ ) and there was no detectable surface conductivity, which reflects the absence of clays or micas.

### 4. Results

[10] Figure 2 shows the measured fluid conductivity perturbations  $\Delta\sigma(t) = \sigma(t) - \sigma_0$ , where  $\sigma_0$  is the conductivity of the primary fluid, for both the upstream (solid circles) and downstream (open circles) reservoirs during two experiments using the S4M and NE34 sands. Note that to compare the results of the different experiments (the sand permeability and, therefore, the flowrate varied between runs owing to slight differences in sand compaction), we normalized the time by dividing it by the time needed by the front to reach the downstream reservoir (neglecting the hydrodynamic dispersion)  $t_Y = \nu Y$ , where  $Y = 31$  cm, and  $\nu$  is the mean fluid velocity. In both experiments, the values measured in the upstream reservoir are in good agreement with theoretical values (continuous lines) obtained from  $\Delta\sigma(t) = (\sigma_p - \sigma_0) \exp(-qt/V_{up})$ , an equation derived from

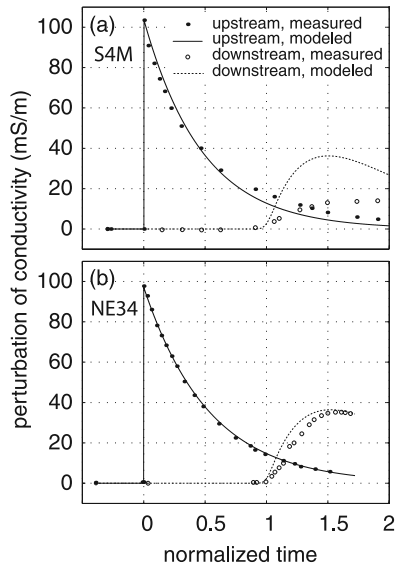


**Figure 2.** Conductivity in the reservoirs. Observed (dots) and predicted (lines) variations of the fluid electrical conductivity in the upstream and downstream reservoirs versus normalized time for the (a) S4M and (b) NE34 experiments.

mass conservation [Maineult *et al.*, 2004], where  $\sigma_p$  denotes the upstream fluid conductivity just after the KCl injection,  $q$  the flowrate ( $\text{m}^3 \text{s}^{-1}$ ),  $t$  the elapsed time after injection (s), and  $V_{up}$  the water volume in the upstream reservoir ( $\text{m}^3$ ). In the downstream reservoir,  $\Delta\sigma$  started to increase only after the KCl front arrived at the downstream reservoir (at  $t = t_Y$ ), reached a maximum, and then slowly decreased (Figure 2). The maximum of the downstream  $\Delta\sigma$  for the S4M experiment (Figure 2a) occurs at a later normalized time and is 2.5 times smaller than for NE34 (Figure 2b). The significance of this difference will be discussed in section 5.

[11] The results of one KCl front experiment in S4M sand are shown in Figure 3a. The primary fluid was deionized water with a small NaCl content ( $\sigma_0 = 8.5 \text{ mS m}^{-1}$ ,  $\sigma_p = 112 \text{ mS m}^{-1}$  and  $\sigma_p - \sigma_0 = 103.5 \text{ mS m}^{-1}$ ). The flow rate  $q$  was equal to  $46 \text{ cm}^3 \text{ min}^{-1}$  ( $v = 4.36 \cdot 10^{-5} \text{ m s}^{-1}$ ). Figure 3a shows the EPD curves versus normalized time (here,  $t_Y = 118.4$  minutes). We observe a simultaneous and identical drop in all the EPDs at  $t = 0$  to a minimum value around  $-7 \text{ mV}$  followed by a slow increase. Afterwards, the EPDs successively jumped back to zero (and over zero) at sequential times in good agreement with the theoretical arrival times of the front at the electrodes (respectively 0.16, 0.39, 0.61 and 0.84 in normalized time, indicated by the vertical lines in Figure 3). The jumps were followed by broad and large (up to  $5 \text{ mV}$ ) overshoots, whose size increased significantly with distance from the upstream reservoir, and ending with a slow return to a stabilized value around  $-1 \text{ mV}$ . Other S4M experiments were performed using tap water ( $\sigma_0 \approx 45 \text{ mS m}^{-1}$ ,  $\sigma_p \approx 145 \text{ mS m}^{-1}$ ). The EPDs exhibited a very similar shape, although the amplitude of the negative part was smaller (around  $-5 \text{ mV}$ ).

[12] For the pure quartz sand experiment shown in Figure 3b, tap water served as primary fluid, with  $\sigma_0 = 46 \text{ mS m}^{-1}$ ,  $\sigma_p = 143 \text{ mS m}^{-1}$  and  $q = 34.6 \text{ cm}^3 \text{ min}^{-1}$

(thus  $v = 3.4 \cdot 10^{-5} \text{ m s}^{-1}$ ,  $t_Y = 151.8 \text{ min}$ ). The initial drop of the EPDs (Figure 3b) had a magnitude more than 3 times smaller than that in the S4M sand. The decrease rate was rapid at first and then slowed down with time. As before, the EPDs showed a sequence of very sharp increases corresponding to the theoretical arrival times of the concentration front at each particular electrode, followed by a small, very narrow overshoot and, finally, a rapid return to zero. Another NE34 experiment ( $q \approx 42 \text{ cm}^3 \text{ min}^{-1}$ , same  $\sigma_0$  and  $\sigma_p$ ) gave similar results.

## 5. Discussion

[13] Maineult *et al.* [2004] devised a conservative model (i.e., without chemical reactions) to compute the downstream conductivity variation  $\Delta\sigma$ . The results of this model are represented by the dotted lines in Figure 2. Experimental data and model are in agreement for the pure quartz sand only (Figure 2b). For S4M sand, the model overestimates the maximum by a factor 2. This observed deficit in conductivity suggests that potassium chloride interacted with some of the minor phases contained in S4M sand but not present in NE34 sand. Experiments on S4M using NaCl [Maineult *et al.*, 2005] exhibited a similar but much smaller effect (the predicted maximum of  $\Delta\sigma$  in the downstream reservoir was less 20% higher than observed); moreover, in the NaCl case, the SP signals did not exhibit positive humps as in Figure 3a. Therefore, we rule out  $\text{Cl}^-$  as main reacting species and conclude that the chemical processes had to involve the  $\text{K}^+$  ions.

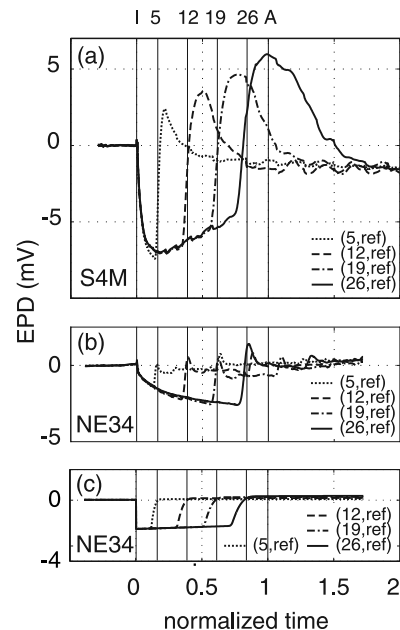


**Figure 3.** Electrical potential differences. Measured EPDs versus normalized time for the (a) S4M and (b) NE34 experiments, and (c) modeled EPDs for the NE34 experiment. The vertical lines labeled I, 5, 12, 19, 26 and A indicate the injection time and the computed arrival times at the sand electrodes and downstream reservoir, respectively. The numbers in parentheses indicate the position of the measurement electrode (the reference electrode is denoted by “ref”).



[14] *Maineult et al.* [2004, 2005] constructed a conservative model for the SP response to the advective transport of concentration fronts (note that the fluid concentration in the sand-body and its evolution with time must first be determined [for details see *Maineult et al.*, 2004, 2005]). This model was validated by comparison with the results of NaCl advection experiments in S4M sand. As briefly explained in section 2, the electrical potential difference  $\Delta U(y_e, t)$  between an electrode located at  $y_e$  and the reference electrode is the sum of two terms:

$$\Delta U(y_e, t) = \Delta U_j(y_e, t) + [\Delta U_e(y_e, t) - \Delta U_e(y_e, 0)] \quad (4)$$

where  $\Delta U_j(y_e, t)$  denotes the junction potential contribution, which is obtained by integrating equation (3) between 0 and  $y_e$ :

$$\Delta U_j(y_e, t) = \int_0^{y_e} \alpha^* \frac{1}{C} \frac{\partial C(y, t)}{\partial y} dy = \alpha^* \ln \frac{C(y_e, t)}{C_{up}(t)} \quad (5)$$

where  $C_{up}$  is the KCl concentration in the upstream reservoir (precautions have to be taken to express this equation as a function of the conductivity [see *Maineult et al.*, 2005]). The bracketed term corresponds to the electrokinetic contribution, and is obtained by integration of equation (1):

$$\Delta U_e(y_e, t) - \Delta U_e(y_e, 0) = \nabla H \int_0^{y_e} (L^*(y, t) - L^*(y, 0)) dy \quad (6)$$

(Note that the incorrectly typed equation (11) given by *Maineult et al.* [2005] should be identical to this last equation). Numerical computation of the integral in equation (6) requires knowledge of the relation  $L^*(\sigma(y, t))$ , which we experimentally estimated on S4M and NE34 samples using the device and procedure described by *Jouniaux et al.* [2000]. For each sand, we used as circulating solutions the same primary fluid as in the advection experiments described above (i.e., tap water for NE34 and deionized + 30 mg L<sup>-1</sup> NaCl for S4M) to which 0, 250 or 500 mg L<sup>-1</sup> KCl were added. Prior to the measurements, we circulated these solutions in a closed-circuit for a sufficiently long time to reach chemical equilibrium. In accordance with equation (1), which predicts that  $L^*$  is inversely proportional to  $\sigma$ , we determined that  $L^* = -1.7 \cdot 10^{-4} \sigma^{-1}$  (in V m<sup>-1</sup>) in the range 0.05 to 0.15 S m<sup>-1</sup> for NE34 and  $L^* = -2.8 \cdot 10^{-4} \sigma^{-1}$  in the range 0.005 to 0.1 S m<sup>-1</sup> for S4M. Then, after solving the conservative transport problem for KCl using the method of *Maineult et al.* [2004, 2005], we computed the EPDs from equation (4) for the NE34 sand (Figure 3c). A perfect match is not obtained. The model predicts sharp, angular EPD curves at  $t = 0$  whereas the observed ones are rounded. Also, the small, narrow overshoots are not reproduced in the theoretical EPDs. However, the model successfully predicts the moderate amplitude of the signals, suggesting that, to first order, the EPDs are dominated by the junction potential (the electrokinetics contribution, not shown here, represents less than 2% of

the total potential). Note that the initial rounding of the EPDs, not predicted by our model, was also observed in all our previous experiments when the reference electrode was placed in the upstream reservoir, irrespective of the electrolyte used [e.g., *Maineult et al.*, 2005]. The general occurrence of this effect suggests that it is more likely caused by insufficient precision of the concentration modeling rather than by the SP model itself. In the aforementioned previous experiments, we also always observed narrow peaks accompanying the passage of the concentration front (just before or just after) but their magnitude (0.3 to 0.6 mV) was much smaller than the overshoots of Figure 3a. Application of our conservative SP model to S4M (using the appropriate value for  $L^*$ ) produces a response similar to those shown in Figure 3c and thus disagreeing completely with the observations. The fact that the model is somewhat successful in the case of pure quartz sand NE34 but fails totally in S4M suggests that the minor mineralogical phases present in S4M (but absent in NE34) must be responsible for this effect.

[15] Based on the two observations above (i.e., deficit of downstream conductivity and failure of the SP model for the S4M sand) we propose that chemical reactions with the minor minerals in S4M sand likely occurred, leading to trapping of K<sup>+</sup> during the passage of the concentration front and their release during passage of the tail. Prior examination of the virgin S4M sand using a binocular magnifying glass showed that the mica grains were essentially biotite, and, to a much smaller degree, muscovite. A new examination, carried out after the NaCl transport experiments of *Maineult et al.*'s [2004, 2005] were performed (but before the KCl ones), revealed that the biotite grains had been altered. It is well known that, during weathering alteration, biotite is chloritized by potassium release [e.g., *Mitchell and Taka*, 1984, and references herein] and that this reaction is quite rapid [*Craw*, 1981; *Pal*, 1985; *Malmström et al.*, 1996]. During a biotite dissolution experiment in neutral pH conditions, *Malmström et al.* [1996] observed that the K<sup>+</sup> concentration in the fluid remained constant at an equilibrium value (1 mmol L<sup>-1</sup>). The stability of the K<sup>+</sup> concentration was explained by a dynamic equilibration between trapping and releasing of K<sup>+</sup>. In our experiment, the KCl concentration at the front was equal to about 7 mmol L<sup>-1</sup>, i.e. greater than the equilibrium concentration mentioned above. Thus, we imagine that, in experiments reported here, K<sup>+</sup> ions were trapped by chloritized biotites as long as the KCl concentration remained over this critical concentration (around 1 mmol L<sup>-1</sup>). The term  $\ln(C/C_{up})$  in equation (5) therefore decreases and the absolute value of the potential gradient increases more than it would if trapping were absent. This explains the observed enhanced amplitude of the initial drop (compared to the response in pure quartz sand). K<sup>+</sup> trapping also explains the deficit of conductivity in the downstream reservoir. Then, as the front concentration passes below the equilibrium concentration, the trapped potassium ions should be released. Thus  $C$  increases and becomes greater than  $C_{up}$  (more than if releasing were absent) producing the marked change in polarity (i.e., the big positive humps) observed in the SP signals. This effect increases with distance and lasts longer owing to the fading of  $C_{up}$  with time. This releasing may

explain the fact that the maximum of the downstream conductivity was delayed in time (Figure 3a).

## 6. Conclusions

[16] This study experimentally demonstrates that chemically active, mineral phases present in rocks and soils even in small amount can strongly affect the SP response to transport of ionic fronts, although we have not yet determined the precise chemical mechanisms involved in the particular case studied here. The retardation effect illustrated here predominantly affects the junction potential term in the SP signals. In other situations, it has been shown that chemical reactions can modify the electrokinetic term as well. For example, the electrokinetic coupling coefficient was significantly reduced in absolute value, and even changed in sign, during calcite precipitation in sand [Guichet *et al.*, 2006]. Chemical modifications of both fluid and matrix, such as those induced by dissolution/precipitation at high temperature, can also strongly affect the SP response [Bernabé *et al.*, 2003]. The electrokinetic behavior of rocks containing different mineral phases (but without any reactions) can also be quite complicated [Hase *et al.*, 2003].

[17] Despite their importance for field data interpretation (it seems highly probable that chemically active minerals will be present in soils and rocks at any site of interest), the effects of the mineralogical composition of rock and of the chemical reactions between minerals and fluid on the self-potential still remain poorly documented. Many studies focused on the electrokinetic potential of homogeneous media (i.e., nearly pure quartz sand or pure clay powder), and few experiments have been performed to date to study the junction potential in porous media. There is presently not enough information available to accurately predict the SP response in strongly heterogeneous soils and rocks. The incremental approach, i.e., starting from an already well-known system and modifying it gradually, may help to gain understanding on this complex topic.

[18] **Acknowledgments.** This research was supported by CNRS. We thank A. Deleforge, who helped to check the reproducibility of the measurements, F. Huber and G. Morvan (Centre de Géochimie de la Surface, Strasbourg) for X-ray diffraction and SEM analysis of sands. A. M. is grateful to A. Clément, Y. Géraud and M. Zamora for discussions, and to the anonymous reviewer for the very constructive comments.

## References

Ahmad, M. U. (1964), A laboratory study of streaming potentials, *Geophys. Prospect.*, 12, 49–64.

- Bernabé, Y., U. Mok, A. Mainault, and B. Evans (2003), Laboratory measurements of electrical potential in rocks during high-temperature water flow and chemical reactions, *Geothermics*, 32, 297–310.
- Corwin, R. F., and D. B. Hoover (1979), The self-potential method in geothermal exploration, *Geophysics*, 44, 226–245.
- Craw, D. (1981), Oxidation and microprobe-induced potassium mobility in iron-bearing phyllosilicates from the Otago schists, New Zealand, *Lithos*, 14, 49–57.
- Guichet, X., and P. Zuddas (2003), Effect of secondary minerals on electrokinetic phenomena during water-rock interaction, *Geophys. Res. Lett.*, 30(13), 1714, doi:10.1029/2003GL017480.
- Guichet, X., L. Jouniaux, and N. Catel (2006), Modification of streaming potential by precipitation of calcite in a sand-water system: Laboratory measurements in the pH range from 4 to 6, *Geophys. J. Int.*, 166, 445–460.
- Hase, H., T. Ishido, S. Takakura, T. Hashimoto, K. Sato, and Y. Tanaka (2003),  $\zeta$  potential measurements of volcanic rocks from Aso caldera, *Geophys. Res. Lett.*, 30(23), 2210, doi:10.1029/2003GL018694.
- Ishido, T., and H. Mizutani (1981), Experimental and theoretical basis of electrokinetic phenomena in rock-water systems and its applications to geophysics, *J. Geophys. Res.*, 86, 1763–1775.
- Jouniaux, L., M.-L. Bernard, M. Zamora, and J.-P. Pozzi (2000), Streaming potential in volcanic rocks from Mount Pelée, *J. Geophys. Res.*, 105, 8391–8401.
- Lome, B., F. Perrier, and J.-P. Avouac (1999), Streaming potential measurements: 1. Properties of the electrical double layer from crushed rocks, *J. Geophys. Res.*, 104, 17,857–17,877.
- Mainault, A., Y. Bernabé, and P. Ackerer (2004), Electrical response of flow, diffusion and advection in a laboratory sand-box, *Vadose Zone J.*, 3, 1180–1192.
- Mainault, A., Y. Bernabé, and P. Ackerer (2005), Detection of advected concentration and pH fronts from self-potential measurements, *J. Geophys. Res.*, 110, B11205, doi:10.1029/2005JB003824.
- Mainault, A., Y. Bernabé, and P. Ackerer (2006), Detection of advected, reacting redox fronts from self-potential measurements, *J. Contam. Hydrol.*, 86, 32–52.
- Malmström, M., S. Banwars, J. Lewenhagen, L. Duro, and J. Bruno (1996), The dissolution of biotite and chlorite at 25°C in the near-neutral pH region, *J. Contam. Hydrol.*, 21, 201–213.
- Mitchell, J. G., and S. Taka (1984), Potassium and argon loss patterns in weathered micas: Implications for detrital mineral studies, with particular reference to the triassic palaeogeography of the British Isles, *Sediment. Geol.*, 39, 27–52.
- Naudet, V., and A. Revil (2005), A sandbox experiment to investigate bacteria-mediated redox processes on self-potential signals, *Geophys. Res. Lett.*, 32, L11405, doi:10.1029/2005GL022735.
- Ogilvy, A. A., M. A. Ayed, and V. A. Bogoslovsky (1969), Geophysical studies of water leakages from reservoirs, *Geophys. Prospect.*, 17, 36–62.
- Pal, D. K. (1985), Potassium release from muscovite and biotite under alkaline conditions, *Pedologie*, 35(2), 133–146.
- Suski, B., E. Rizzo, and A. Revil (2004), A sandbox experiment of self-potential signals associated with a pumping test, *Vadose Zone J.*, 3, 1193–1199.

Y. Bernabé and L. Jouniaux, Institut de Physique du Globe de Strasbourg, CNRS UMR 7516, Université Louis Pasteur, 5 rue Descartes, F-67000 Strasbourg, France.

A. Mainault, Institut de Physique du Globe de Paris, 4 place Jussieu, F-75005 Paris, France. (mainault@ipgp.jussieu.fr)